

Influence of rainfall on wind power generation in Northeast Brazil Influência da precipitação na geração de energia eólica no Nordeste do Brasil

Alessandra Maciel de Lima Barros¹ , Maria do Carmo Martins Sobral² , Janaina Maria Oliveira de Assis² ,
Werônica Meira de Souza³ 

ABSTRACT

Wind power has been emerging as one of the main renewable energy sources in Northeast Brazil, which concentrates 87% of the country's installed wind capacity, especially in recent years, due to water scarcity and its seasonal energy complementarity to hydraulic generation. The objective of this article is to present a method to evaluate the influence of rainfall on the behavior of wind power generation, considering rainfall anomaly index and extreme climatic indices of precipitation. We utilized daily rainfall data from cities located near wind farms CE1 and CE2 in the state of Ceará — Aracati, in the 1974-2016 period, and Trairi, in the 1976-2016 period —, as well as daily wind power generation data for the same period, provided by the Electric System National Operator (ONS). The RCLimindex software was used to calculate 11 indices of climatic extremes dependent on rainfall. The capacity factor for wind power generation was calculated for the period from 2011 to 2016 for the CE1 and CE2 wind farms. The application of this method found an inversely proportional relation between rainfall anomaly index (RAI) and the wind power capacity factor, with a decrease in total rainfall and a greater number of consecutive dry days and concentrated rain in the short term. From 2012 to 2016, the rainfall anomaly index was negative. However, wind power factors were higher than in 2011. The developed methodology can be applied to other wind farms, contributing to the medium and long term energy planning of the National Interconnected System.

Keywords: extreme events; energy planning; wind power factor; RCLimindex.

RESUMO

A energia eólica vem despontando como uma das principais fontes renováveis de energia no Nordeste do Brasil, que concentra 87% da capacidade eólica instalada no país, especialmente nos últimos anos, devido à escassez hídrica e à sua complementariedade energética sazonal à geração hidráulica. O objetivo deste artigo é apresentar um método para avaliar a influência da precipitação no comportamento da geração de energia eólica. Foram utilizados dados diários de precipitação pluviométrica de cidades localizadas perto das usinas eólicas CE1 e CE2 no estado do Ceará — Aracati, no período 1974-2016, e Trairi, no período 1976-2016 —, bem como dados diários de geração eólica do mesmo período, fornecidos pelo Operador Nacional do Sistema Elétrico (ONS). Utilizou-se o software RCLimindex para calcular 11 índices de extremos climáticos dependentes da precipitação pluviométrica. Com isso, determinou-se o fator de capacidade de geração de energia eólica para o período de 2011 a 2016 nas estações eólicas CE1 e CE2. A aplicação desse método constatou a existência de uma relação inversamente proporcional entre o Índice de Anomalia de Chuva (IAC) e o fator de capacidade da geração de energia eólica, com predominância de tendência de diminuição da precipitação total, com maior número de dias secos consecutivos e chuvas concentradas em curto período de tempo, embora os fatores eólicos tenham sido superiores a 2011. A metodologia desenvolvida pode ser aplicada a outros parques eólicos, contribuindo para o planejamento energético de médio e longo prazo do Sistema Interligado Nacional.

Palavras-chave: eventos extremos; planejamento energético; fator de capacidade da geração eólica; RCLimindex.

¹Operador Nacional do Sistema Elétrico – Rio de Janeiro (RJ), Brazil.

²Universidade Federal de Pernambuco – Recife (PE), Brazil.

³Universidade Federal do Agreste de Pernambuco – Garanhuns (PE), Brazil.

Correspondence address: Alessandra Maciel de Lima Barros – Rua José Higino, 221, ap. 1.203 – Madalena – CEP: 50610-340 – Recife (PE), Brazil – E-mail: maciel.alessandra@gmail.com

Conflicts of interest: the authors declare that there are no conflicts of interest.

Funding: Brazilian National Council for Scientific and Technological Development (CNPq).

Received on: 04/24/2020. Accepted on: 01/06/2021

<https://doi.org/10.5327/Z21769478769>



This is an open access article distributed under the terms of the Creative Commons license.

Introduction

Annually, more than 19,000 billion kWh of electricity are produced worldwide. About 70% comes from burning fossil fuels (41.5% from coal), followed by hydroelectric, nuclear, and other sources. One of the great challenges of the global energy sector is to satisfy the increased demand for energy, diversifying the energy matrix in order to reduce greenhouse gas emissions. In this context, the importance of renewable sources in the world energy matrix is growing. At least 45 countries, including 10 developing countries, have political goals to increase their use of renewable energy sources (GWEC, 2010).

Since 2014, Brazil is on the list of the 10 countries in the world with the largest installed capacity of wind energy, and has become a leader in the wind energy market in South America (GWEC, 2016). In 2019, the country reached a total of more than 15 GW of installed capacity. In 2024, Brazil's installed wind capacity will increase to 19 GW, representing an 11.1% growth from 2019 to 2024 (ONS, 2020). These values refer to the installed capacity onshore. Luz et al. (2020) point out that offshore wind projects are less impactful to the environment than onshore ones. So far, there are no plans to install offshore wind farms in Brazil.

Wind power has numerous benefits that make it an attractive energy source for both large energy consumers and small production applications distributed. The main benefits of this type of energy include: clean and inexhaustible energy; modular and scalable technology; energy price stability; reduced dependence on imported fuels; and economic development (Reeves and Beck, 2003).

Renewable energy, represented by small hydroelectric, biomass, wind, and solar plants, encompasses options to diversify the Brazilian electric matrix. However, it should not be seen only as an environmentally sustainable choice for a clean generation system, but also as an approach that addresses other social needs. Among these needs, there is greater reliability and security of supply, promoting seasonal energy complementarity to hydraulic energy — responsible for the largest portion of the installed capacity of electricity generation in the country —, improvement of maintenance of energy security, decrease in environmental impacts resulting from the use of fossil fuel, and reduction of climate change (Brasil, 2009; Wang et al., 2018).

Wind power generation cannot be addressed without discussing the issue of climate change, since it has caused changes in temperature and rainfall in different regions, with emphasis on the Northeastern region of Brazil, which has a high degree of climate vulnerability (Brasil, 2007). A warmer atmosphere is estimated, with more occurrences of extreme events of drought and rainfall, in frequency and intensity, causing more recurrent droughts and more severe floods (Marengo, 2007).

The consumption of fossil fuels has been increasing over the years and, along with them, the increase in greenhouse gases in the atmosphere has also been greater. However, in order to avoid environmental degradation, the use of renewable energy sources has increased visibly

in recent years. Incentives were created for the production of renewable energy by the European Union, which, in July 2007, decided to reduce greenhouse gas emissions by 20%, increase the use of renewable energy systems by 20%, as well as increase energy efficiency by 20% by the end of 2020 (Ribeiro et al., 2014).

Climate change puts enormous pressure on water resource management. Floods and their consequences and severe droughts are resulting in natural disasters that reduce or destroy people's livelihoods in many regions of the world (Munichre, 2017). There has been a considerable increase in extreme weather events that cause deaths, economic loss, and destruction of infrastructure over the last decades, in addition to major impacts on energy generation (Souza et al., 2014).

In different regions of South America, extreme weather events have become increasingly common. The great droughts that occurred in the Amazon, from 2005 and 2010 (Lewis et al., 2011) and the great floods of 2008/2009 (Marengo et al., 2012), 2012 (Espinoza et al., 2013), and 2014 (Espinoza et al., 2014) can be mentioned, as well as the drought in Southeast Brazil in 2014/2015 (Coelho et al., 2016). According to the Fifth Assessment Report of the Intergovernmental Panel on Climate Change (IPCC AR5), published in 2013, climate change has been observed across the planet. Marengo (2008) points out that changes in rainfall patterns deserve great prominence among the observed climate changes, considering that they may change the availability of rain in one region or another. To verify these changes, indicators of climatic extremes, which indicate the intensity and frequency of such extreme events across the globe, can be used (Sillmann et al., 2013a).

In this context, the analysis of the influence of rainfall on the behavior of wind power generation is essential to guarantee a more robust forecast in the short and medium terms, particularly in the coast of Northeast Brazil, which concentrates 87% of the country's installed wind capacity, being one of the regions with the greatest potential for wind power generation in Brazil.

Thus, the present article aims to analyze the extreme climatic indices of rainfall in the state of Ceará, as well as rainfall anomaly index and its relation with the behavior of wind power generation through the analysis of the existing correlation between the capacity factor and rainfall anomaly index.

Climate change process

The Northeastern region of Brazil faces serious problems related to rainfall irregularity, resulting in severe and prolonged droughts, as well as extreme rainfall and floods (Ferreira et al., 2017). In this region, events like La Niña have been associated with the occurrence of rainy seasons that are more humid than normal, whereas El Niño has been associated with the occurrence of seasons drier than normal (Rodrigues et al., 2017). Many renewable energy sources for electricity generation, such as hydroelectric and wind power, depend on climatic factors. In the Northeastern region of Brazil, the installed capacity of wind power generation has increased substantially in recent years. The planned fu-

ture increase in installed wind power capacity may change this picture; the demand for electricity generated by thermoelectric and imported plants will decrease (Koch et al., 2018).

According to Souza (2010), when choosing energy generation alternatives, the focus on sustainable development becomes necessary. Issues related to air pollution, greenhouse effect, depletion of fossil fuel reserves, security of supply, and equity are some of the drivers.

Managing the variability of wind power is a key factor in minimizing the cost of integrating wind-based power generation into grid systems, while maintaining the extremely high level of reliability required. The short-term forecast for wind energy is that it is one of the most economical and easy to implement investments available to system operators (Zack et al., 2016).

Several meteorological systems affect the climate in the Northeastern region of Brazil. The Intertropical Convergence Zone (ITCZ) is one of the systems that govern the rainfall trend in the northern part of the Northeastern region of Brazil. The ITCZ reaches its position further south between February and April, and further north between August and October (Oliveira and Costa, 2011). In addition to this annual oscillation, it presents oscillations with higher frequencies, varying from weeks to days. The influence of this positioning on rainfall is addressed in several studies (Lyra et al., 2019). The ITCZ is more significant over the oceans, and therefore, Sea Surface Temperature (SST) is one of the determining factors in its position and intensity (Ferreira and Mello, 2005; Carvalho, 2020).

The seasonal variation of ITCZ's positioning influences the generation of wind energy. In their analysis, Barros et al. (2017) found that the variation of ITCZ's position negatively influenced wind generation in the state of Ceará in February 10 and 11, 2017. In these days, wind generation was practically zero at some points of the day. Due to the high installed capacity of wind farms in the Northeastern region of Brazil, understanding the influence of meteorological systems on the behavior of wind generation is of fundamental importance for the operation of the electrical system.

Wind power generation in Brazil and in the Northeastern region of the country

The National Interconnected System (*Sistema Interligado Nacional* – SIN) is a hydro-thermo-wind system of continental dimensions, with an installed capacity of more than 162 GW, with 83% of the generation coming from renewable sources (hydroelectric + wind + solar), of which about 73% are hydraulic plants, which makes Brazil a world reference in renewable energy.

The Brazilian generating complex is undergoing a process of transformation and transition. Hydroelectricity will continue as the main source of energy generation, although its share in the total installed power of SIN will be reduced from 66.7%, in 2018, to 62.1%, in 2024 (ONS, 2020). Inserting future wind farms in SIN will promote beneficial effects for the entire system, espe-

cially for the Northeastern region, where the complementarity of wind generation in relation to the period of low inflows is registered.

In Brazil, SIN's installed generation capacity is mainly composed of hydroelectric plants distributed in 16 drainage basins, in different regions of the country. In recent years, the installation of wind farms, mainly in the Northeastern and Southern regions, has grown considerably, increasing the importance of this generation for serving the market. Due to the increase in the installed capacity of wind generation since 2014, its participation has grown over the years. In 2019, wind and solar generation served 10% of the SIN load, hydraulic generation served 73%, and thermal generation served 17%.

Since 2016, wind generation has been serving the highest percentage of the load in the Northeast, with its peak in 2019, when it served 50% of the load. Despite the water crisis, the Northeast exported roughly 1,500 MWmed from July to December 2019. The growth in the share of the solar source is also remarkable in the last three years, meeting 3% of the demand in the Northeast in 2019 (ONS, 2020).

Material and Methods

The method used to assess the influence of rainfall on the behavior of wind power generation was based on the consideration of the rainfall anomaly index and its relation with the capacity factor, as well as the assessment of extreme climatic precipitation indices, considering the following steps.

Selection of the study area

To select the study area, we sought a region in the Northeast with a large number of wind farms in operation, as well as pluviometric stations close to wind farms with good quality historical series available.

The coast of the state of Ceará was selected, as it has several wind farms in commercial operation with potential for expansion. The existence of nearby pluviometric stations with available historical series is also important. The plants in the coastal region of the state of Ceará were grouped into two located groups (CE1 and CE2), which have a higher concentration of plants, as shown in Figure 1.

Wind power plants (CE1 and CE2) were selected in two different areas of the coast of the state of Ceará, as they are representative of the plants operating on the northeastern coast. Trairi and Aracati rain stations were selected, due to the proximity to the selected wind farms, CE1 and CE2, respectively. The selection was made after analyzing the distance between the selected wind farms and the automatic meteorological stations of the National Institute of Meteorology (INMET) and Ceará's Foundation for Meteorology and Water Management (FUNCEME), as well as the National Water Agency's (ANA) rainfall stations (Brasil, 2016).

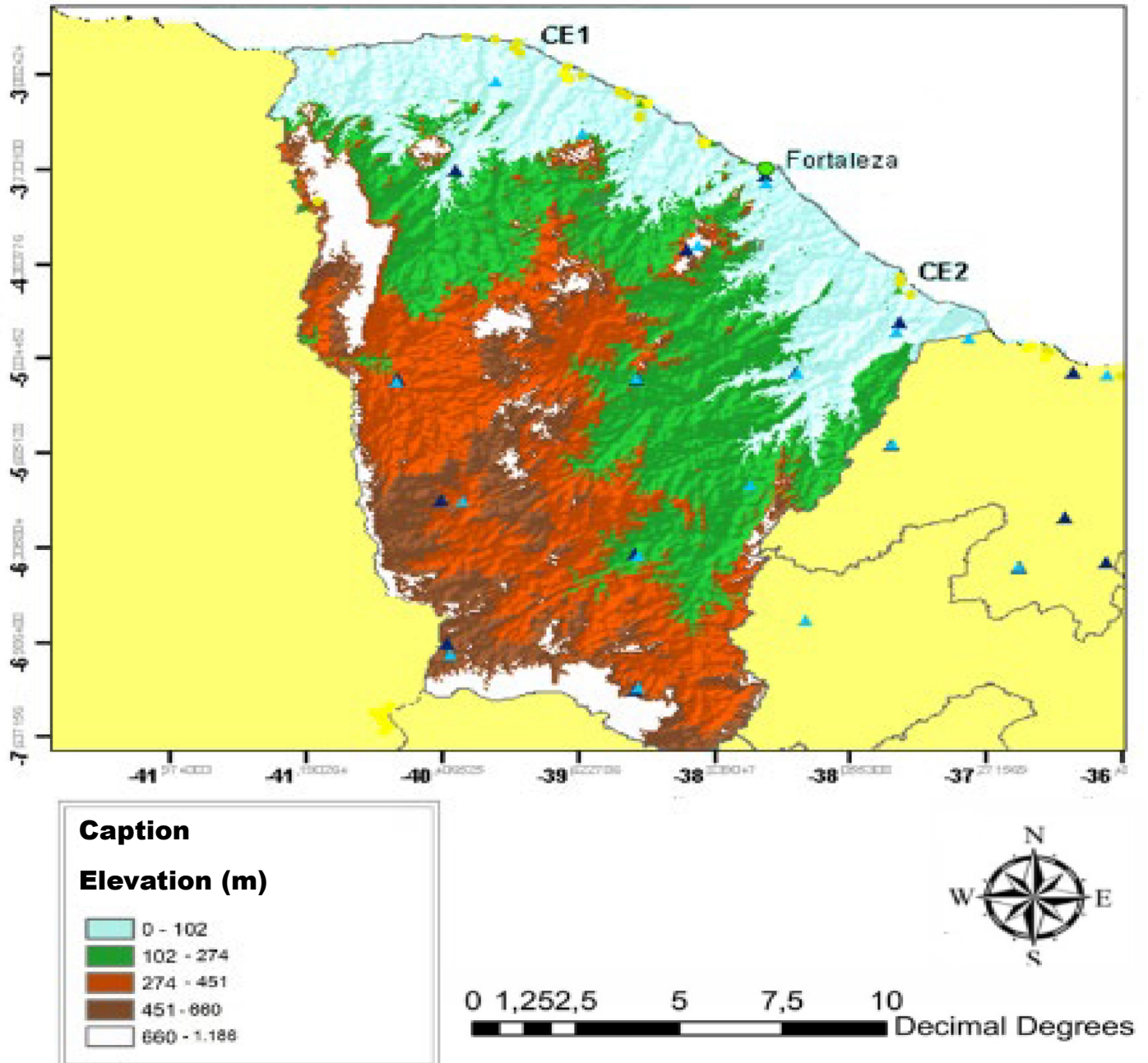


Figure 1 - Digital elevation map and location of wind farms in the state of Ceará.
Source: created with data from ONS (2020) and IBGE (2011).

Treatment and analysis of rainfall data

The consistency of the historical series and the filling of gaps in the daily rainfall data were performed using the simple linear regression method, which correlates the gaps in the station and in a neighboring station with gaps, as proposed by Tucci (2004).

The series consistency analysis was performed using the double mass method, developed by the United States Geological Survey (USGS), commonly adopted in Brazil. The methodology consists of selecting stations in a region and accumulating the monthly values for each of them. Then, the accumulated values corresponding to the

station to be validated (in ordinates) and to another reliable station adopted as a basis for comparison (abscissa) were plotted on a Cartesian graph. With this method, identifying systematic errors (change in slope or trend), transcription errors, or stations subject to different rainfall regimes is possible (Tucci, 2004).

Rainfall Anomaly Index

Rainfall anomaly index (RAI) analyzes the frequency of dry and rainy years and the intensity of events. Based on Van-Rooy's methodology (1965) and adapted to the Northeast of Brazil by Freitas (2005), the climatic variability is evaluated through the creation of climatic indices spatialized in time and space, detecting periods considered extremely humid or dry. The assessment of the degree of severity and duration of the dry and wet periods was carried out by calculating the RAI (Freitas, 2005), obtained from Equations 1 and 2:

$$IAC = 3 \left[\frac{(N - \bar{N})}{(M - \bar{N})} \right], \text{ for positive anomalies} \quad (1)$$

$$IAC = -3 \left[\frac{(N - \bar{N})}{(\bar{X} - \bar{N})} \right], \text{ for negative anomalies} \quad (2)$$

Where:

N = annual precipitation (mm);

\bar{N} = average annual precipitation of the historical series (mm);

M = average of the 10 largest annual rainfall in the historical series (mm);

\bar{X} = average of the 10 lowest annual rainfall in the historical series (mm).

Positive anomalies are values above the historical average and negative anomalies are below the historical average of precipitation. Based on the methodology proposed by Freitas (2005) and Araújo et al. (2009), the classification of dry and wet years was used as a climatic indicator for the intensity of these anomalies, as shown in Table 1.

The average monthly rainfall was calculated with the history of the selected weather stations for January to May, from 2011 to 2016.

Wind generation capacity factor

In the present study, the capacity factor used is understood as a function of wind generation. The capacity factor of wind power generation is calculated through the relation between the average wind power generation and the installed capacity of the wind power plant, as shown in Equation 3.

$$FC = \left[\frac{(EOL \text{ generation } (MW_{med}))}{\text{Installed Capacity } (MW)} \right] \quad (3)$$

Power generation is a function of wind speed, whose behavior varies over the day and over the months. The topographic characteristics of a region also influence the behavior of winds, since, in certain areas, differences in speed may occur, causing a reduction or acceleration in wind speed (Custódio, 2009). Among the main influencing factors in the wind regime, the following stand out: variation in speed with

height; terrain roughness, which is characterized by vegetation, land use, and occupation; presence of obstacles in the vicinity; and the terrain, which can cause an effect of acceleration or deceleration in air flow (Varejão-Silva, 2006).

Calculation of extreme rainfall climate indices

With the purpose of detecting trends of climatic extremes indices in the analyzed stations, the software RCLimindex 3.2.1, which is a program recommended by the World Meteorological Organization (WMO) for the calculation of climatic extremes indices aiming at monitoring and detecting climate changes, was used. This software was developed in R by Byron Gleason, a researcher at the National Oceanic and Atmospheric Administration's National Climate Data Center (NCDC), and has recently been used in CCI/CLIVAR (International Research Programme Climate Variability and Predictability) climate index workshops, according to Karl et al. (1999).

RCLimindex 3.2.1 calculates all 27 basic indexes (11 related to precipitation and 16 related to temperature) recommended by the Expert Team on Climate Change Detection Monitoring and Indices (ETCCD-MI) and provides, for each calculated index, statistical information, such as linear trend calculated by the method of least squares, level of statistical significance of the trend (p value), coefficient of determination (R^2), and standard error of the estimate, in addition to the graphs of the annual series (RCLIMDEX, 2004). In this work, only the 11 indices derived from rainfall were used, as shown in Table 2.

The climatic indices can be used to create graphs of the annual series, composed by the trends and calculated by the method of linear least squares regression, with statistical significance, showing the adjustments of these linear trends to the graphs statistically.

Rainfall and wind generation data used

The data from the 1974-2016 period from Aracati station, as well as data from 1976 to 2016 from Trairi station, was used. Daily wind generation data for 2011 to 2016, provided by ONS for the wind farms CE1 and CE2, were also used.

Table 1 – Intensity levels of rainfall anomaly index (RAI).

RAI Range	Intensity Level
Above 4	Extremely humid
2 to 4	Very humid
0 to 2	Humid
0 to -2	Dry
-2 to -4	Very dry
Below -4	Extremely dry

Source: Freitas (2005).

Table 2 – Climatic indices depending on daily rainfall with definitions and units.

Index	Indicator Name	Definition	Unit
PRCPTOT	Total annual rainfall on wet days	Total annual rainfall on wet days (RR ≥ 1 mm)	mm
CDD	Consecutive dry days	Maximum number of consecutive days with RR < 1 mm	days
CWD	Consecutive wet days	Maximum number of consecutive days RR ≥ 1 mm	days
R10mm	Number of days with precipitation above 10 mm	Number of days per year when rainfall was ≥ 10 mm	days
R20mm	Number of days with precipitation above 20 mm	Number of days per year when rainfall was ≥ 20 mm	days
R50mm	Number of days with rainfall above 50 mm	Number of days per year when rainfall was ≥ 50 mm	days
SDII	Simple daily intensity index	Total annual rainfall divided by the number of wet days (defined by PRCPTOT ≥ 1 mm)	mm/day
Rx1day	Maximum amount of rainfall in one day	Maximum monthly amount of rainfall in one day	mm
Rx5day	Maximum amount of precipitation over five consecutive days	Maximum monthly amount of rainfall over five consecutive days	mm
R95p	Very humid days	Total annual rainfall in which RR > 95 percentile	mm
R99p	Extremely humid days	Total annual rainfall in which RR > 95 percentile	mm

*RR indicates daily precipitation.

Source: RCLIMDEX 1.0 (2004).

In the analysis of the extreme climatic indices of pluviometric precipitation, the daily observed data from the Trairi pluviometric station, from 1976 to 2015, is considered.

Correlation analysis

Pearson’s correlation was also known as the Product-Moment Correlation Coefficient (Figueiredo Filho and Silva Júnior, 2009). The population correlation coefficient (parameter) ρ and its sample estimate are closely related to the normal bivariate distribution, whose probability density function is given by Equation 4:

$$f_{X,Y}(X, Y) = \frac{1}{2\pi\sigma_X\sigma_Y\sqrt{1-\rho^2}} \exp \left\{ -\frac{1}{2(1-\rho^2)} \left[\left(\frac{X-\mu_X}{\sigma_X} \right) - 2\rho \left(\frac{Y-\mu_Y}{\sigma_Y} \right) + \left(\frac{Y-\mu_Y}{\sigma_Y} \right)^2 \right] \right\} \quad (4)$$

In which:

$$\rho_{X,Y} = \rho = \frac{COV(X,Y)}{\sigma_X\sigma_Y} = \frac{\sigma_{X,Y}}{\sigma_X\sigma_Y} = \text{the population parameter:}$$

COV(X, Y) = the covariance between X and Y;

σ_X = the standard deviation of X;

σ_Y = the standard deviation of Y.

The Maximum Likelihood Estimator is given by Equation 5:

$$\hat{\rho}_{X,Y} = \hat{\rho} = \frac{\sum_{i=1}^n (\rho - \bar{X})(Y_i - \bar{Y})}{n \sqrt{\frac{\sum_{i=1}^n (X_i - \bar{X})^2}{n} \sqrt{\frac{\sum_{i=1}^n (Y_i - \bar{Y})^2}{n}}}} = \frac{\sum_{i=1}^n (X_i - \bar{X})(Y_i - \bar{Y})}{n\hat{\sigma}_X\hat{\sigma}_Y} \quad (5)$$

In which:

n = the number of observations in the sample;

\bar{X} = the arithmetic mean of X;

\bar{Y} = the arithmetic mean of Y;

$\hat{\rho}$ = the standard deviation;

X_i = observation of variable x;

Y_i = observation of variable y.

The correlation coefficient can also be interpreted in terms of ρ² = R², called the determination or explanation coefficient. When multiplied by 100, ρ² = R² gives the percentage of variation in Y (dependent variable), which can be explained by the variation in X (independent variable), that is, how much variation is common to both variables. The determination coefficient is the relation between the variation explained by the linear model (Y[^] = α[^]+β[^]X, in which α[^] and β[^] are constant) and the total variation.

The significance of the correlation coefficient will be assessed using the Student’s t-test, for the significance levels of 1, 5, and 10%, and degrees of freedom of (n-2). Rejections to null hypotheses h0 will identify the existence of a linear correlation between the combinations performed. To test the hypothesis that the linear correlation coefficient is equal to zero, there must be: H0: ρ = 0 and H1: ρ ≠ 0, according to Equations 6 and 7:

$$t = \frac{\hat{\rho}\sqrt{n-2}}{\sqrt{1-\hat{\rho}^2}} \sim t_{n-2} \quad (6)$$

In which:

t₀ = the test statistic;

$\hat{\rho}$ = the standard deviation;

n = the sample size;

r = the estimate of the linear correlation coefficient.

Under the assumption of the null hypothesis $H_0: \rho = 0$. The null hypothesis is rejected if:

$$|t_0| > t_{\alpha/2(n-2)} \tag{7}$$

t_0 = the test statistic;
 n = the sample size;

The correlations that presented statistical significance at the 5% level, obtained by the Pearson method, were discussed. Pearson's correlation method (p) is a measure of linear association between two variables, expressed by Equation 8:

$$= \frac{1}{n-1} \sum \left(\frac{x_i - \bar{X}}{s_x} \right) \left(\frac{y_i - \bar{Y}}{s_y} \right) \tag{8}$$

Significance was obtained with the Student's t-test applied to a series that represents N degrees of freedom, corresponding to the years of the historical series of data analyzed. The significance level (α) is understood as the probability of making a certain estimate wrong. The lower the level of significance, the higher the confidence level ($1 - \alpha$) of the correlation index obtained. For a significance level of $\alpha = 0.005$ (5%), the confidence level is 0.95 (95%). The most frequently confidence level used as a limit for climatology is 95%.

Results and Discussion

Analysis of Rainfall Anomaly Index and its relation with the capacity factor of wind power generation

For the correlation analysis of the IAC \times capacity factor of wind generation, average rainfall was used, calculated using the arithmetic average method, which consists of the average of the records of precipitation values. According to Tucci (2004), this method is influenced by extreme values and is satisfactory when sample distribution is uniform.

Figure 2 shows the capacity factor as a percentage of the wind farm CE2, and the rainfall anomaly index of the Aracati (CE) meteorological station from January to May, 2011 to 2016.

In 2011, the months of January, February, April and May showed positive anomalies in precipitation, and the average capacity factor (CF) of the period was 14%. In 2012, the months from January to May showed negative rainfall anomalies. The average CF of the period was 42%, that is, three times higher than the average CF recorded in 2011. The negative results of the IAC for 2012 are in line with the results obtained by Assis et al. (2015) in the climatic analysis of rainfall in the sub-basin of the São Francisco River basin, based on rainfall anomaly index performed. In their analysis, there was no positive RAI in 2012. All indices were classified as dry and extremely dry.

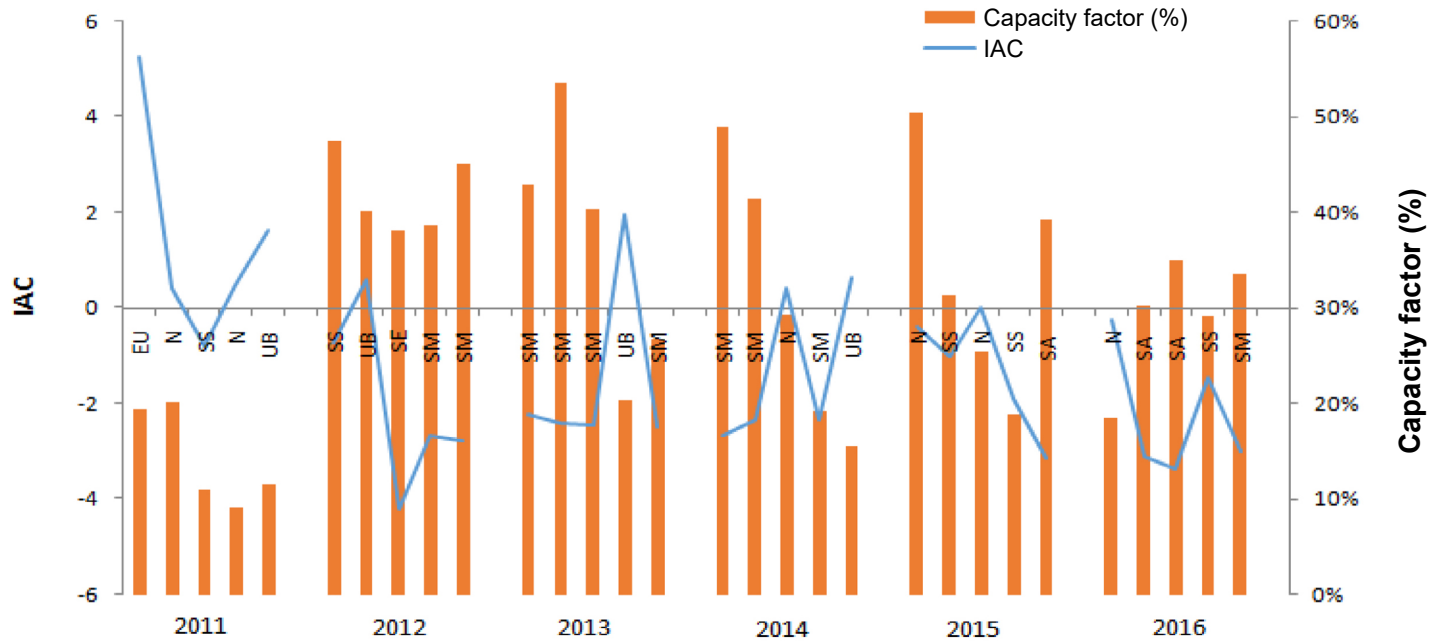


Figure 2 – Relation between the rainfall anomaly index and the capacity factor of wind generation in CE3, from January to May, 2011 to 2016. EH: extremely humid; HH: high humidity; MH: moderate humidity; LH: low humidity; N: normal; MD: mild drought; MD: moderate drought; HD: high drought; ED: extreme drought.

In 2013, the months of January, February, March and May showed negative anomalies in rainfall, and the average capacity factor (CF) of the period was 41%. In April, rainfall anomaly was positive and the CF dropped to 20%. In 2014, the months of January, February and April presented negative rainfall anomaly and the average CF was 37%. In March and May, 2014, with a positive rainfall anomaly, the average CF dropped to 22%.

In 2015, the months of January, February and March presented negative rainfall anomaly and the average CF was 36%. In May, rainfall anomaly was positive and the CF dropped to 39%. In 2016, January presented rainfall anomaly close to the average, with the CF equal to 19%. In the months of February, March, April and May, in which rainfall anomaly was negative, the average CF was 32%.

Figure 3 shows the average RAI for the period from January to May, 2011 to 2016. According to the analysis carried out, the CF tends to be higher in dry years. In the last five years, 2012 to 2016, negative rainfall anomalies with high capacity factors were observed. According to Marengo et al. (2016), the drought that plagued the semi-arid Northeastern region from 2012 to 2015 had an intensity and impact not seen in several decades. Changes in atmospheric circulation and rainfall detected since the summer of 2012 suggest a more active role of surface waters, cooler than the normal in the equatorial Pacific, and an Intertropical Convergence Zone displaced anomalously north from its regular position, with increased subsidence over the Northeastern region of Brazil. In the Northeast of Brazil, signs of drought began to appear in December 2011, and intensified during the summer and autumn of 2012, generating water deficiency in almost the entire semi-arid region, from central-southern Bahia state to the states of Rio Grande do Norte and Ceará in 2011-2014.

id region, from central-southern Bahia state to the states of Rio Grande do Norte and Ceará in 2011-2014.

For the annual analysis of the linear correlation between the rainfall anomaly index (RAI) and the capacity factor (CF), there was a strong negative linear correlation, whose value was -0.87. It shows a reduction in CF in the months with positive rainfall anomalies. Although the period of analysis is short, from 2011 to 2016, this is the history available considering that the plants started their commercial operation in 2010. Despite this limitation, the results obtained are relevant because they present an analysis of rainfall impacts on the behavior of wind generation on the coast of Northeast Brazil. This study may be updated as the historical series is expanded.

According to the analysis carried out, there was a smaller capacity factor in the years that presented positive rainfall anomalies. However, in the years in which rainfall anomaly was negative (rain below the historical average), the capacity factor was higher. The analysis reveals that when the registered rainfall is below the historical average, the capacity factor for generating wind energy increases; on the other hand, when rainfall is above climatology, the capacity factor decreases.

Figure 4 illustrates the relation between the average daily wind generation verified \times observed wind \times observed rainfall of CE1 for the period from 03/29/2014 to 05/30/2016.

On the days in which daily rainfall was higher (above 20 mm), the average daily wind speed was below 6 m/s. As a consequence, wind generation was lower on these days. In this region, the main responsible factor in the occurrence of rainfall is the Intertropical Convergence Zone (Lyra et al., 2019).

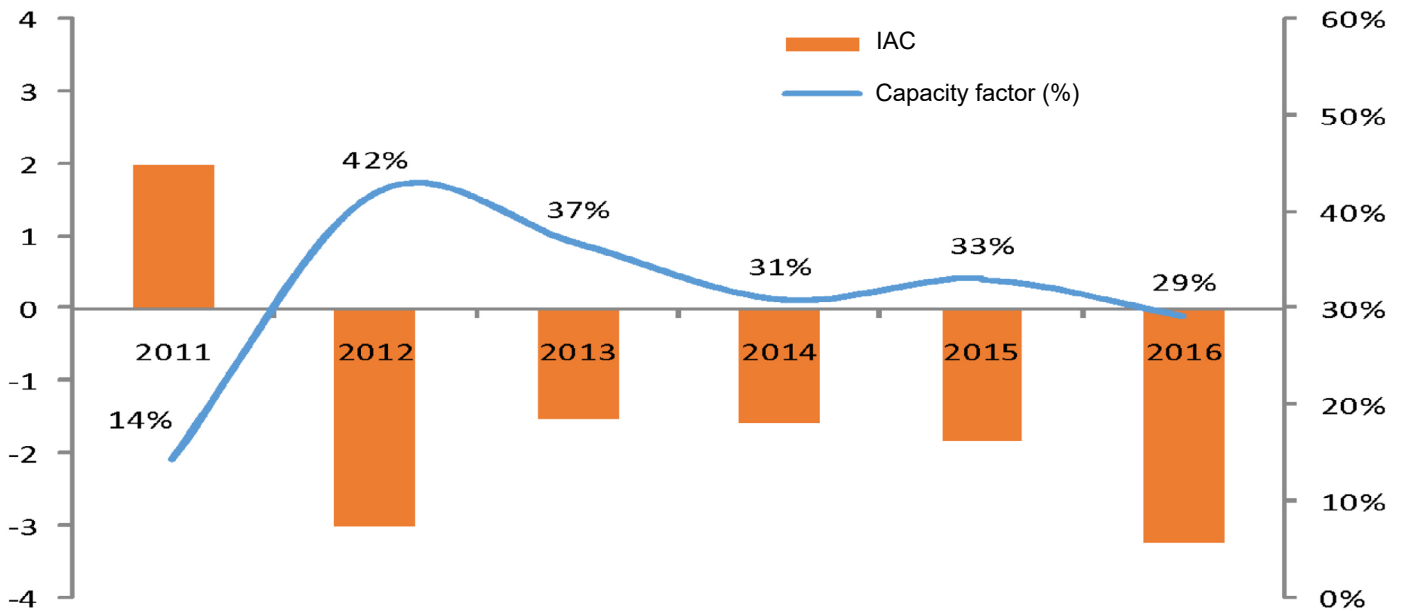


Figure 3 – Rainfall anomaly index for the period from January to May and the average capacity factor for the period.

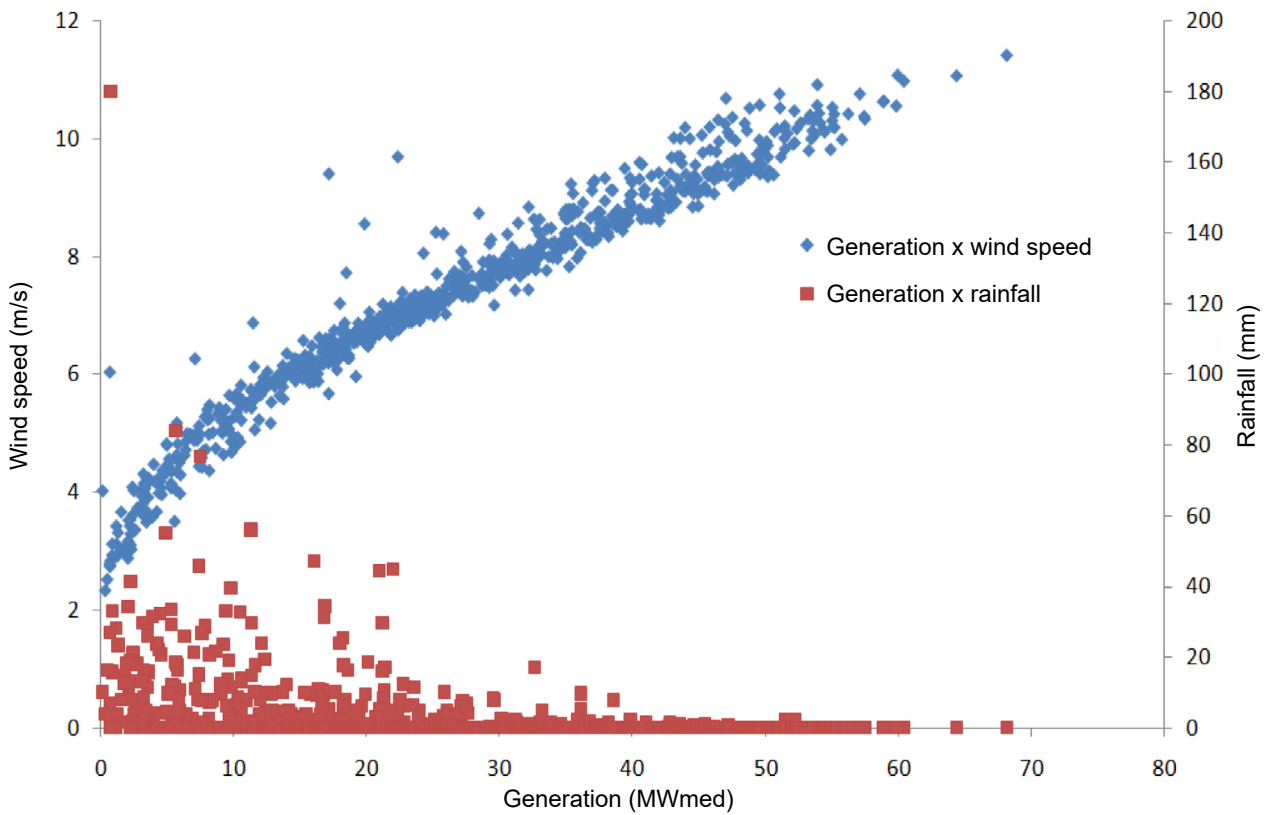


Figure 4 – Relation between wind generation, wind speed, and rainfall (CE1).

Calculation of climatic extremes indices using RCLimindex

The results of climatic extremes indices using RCLimindex are presented below.

Linear trend of total annual rainfall

Figure 5 shows the total annual rainfall index (PRCPTOT) of Aracati station, from 1974 to 2015. According to this index, there is a linear decreasing trend in the annual rainfall pattern. For the analyzed period, annual rainfall reduction rate was 19.7 mm.year⁻¹, that is, a reduction of 862 mm in precipitation over the last 42 years. The years 1983, 1993, 1998, and 2012 had the lowest total rainfall, with 1993 being the most critical year, with a total annual rainfall of 220 mm. The years 1993 and 1998 are associated with the strong-intensity El Niño phenomenon. The year 2012 did not constitute an occurrence of El Niño, however, it was an extremely dry year due to a Sea Surface Temperature (SST) anomaly in the Pacific Ocean (Rodrigues et al., 2017).

Figure 6 shows the total annual precipitation index (PRCPTOT) of the Trairi station. According to this index, there is a linear trend, which is not too sharp, in the annual rainfall pattern. For the analyzed period, the rate of annual rainfall increase was 10.5 mm.year⁻¹, that is, an increase in total annual rainfall of 420 mm over the last 40 years.

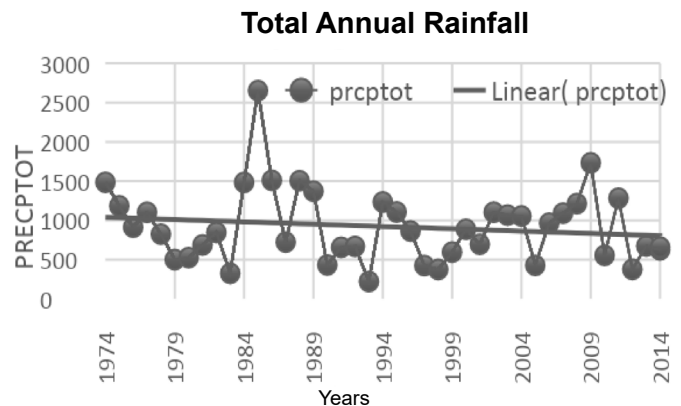


Figure 5 – Linear trend of total annual rainfall (PRCPTOT) of the Aracati station mm/year (1974–2015).

In the analysis of the temporal trend of the PRCPTOT index in Trairi, an alternation between rainy and dry years is observed, with annual rainfall above and below average. The years 1979 and 1993 presented the lowest total rainfall, with a total annual rainfall of 500 mm. The years 1977, 1985, 2002, 2003, and 2009 presented the highest annual rainfall volumes with annual values above 1,500 mm.

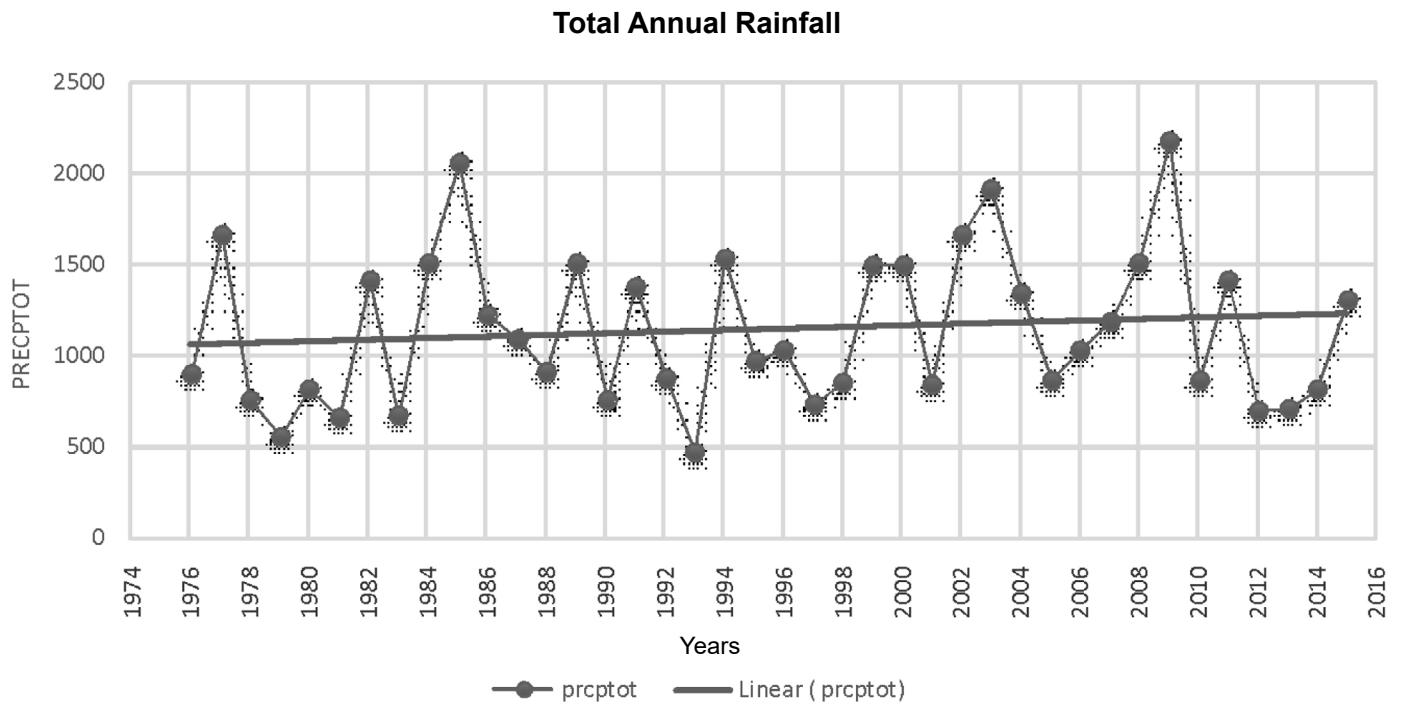


Figure 6 - Linear trend of total annual rainfall (PRCPTOT) of the Trairi station mm/year (1976–2015).

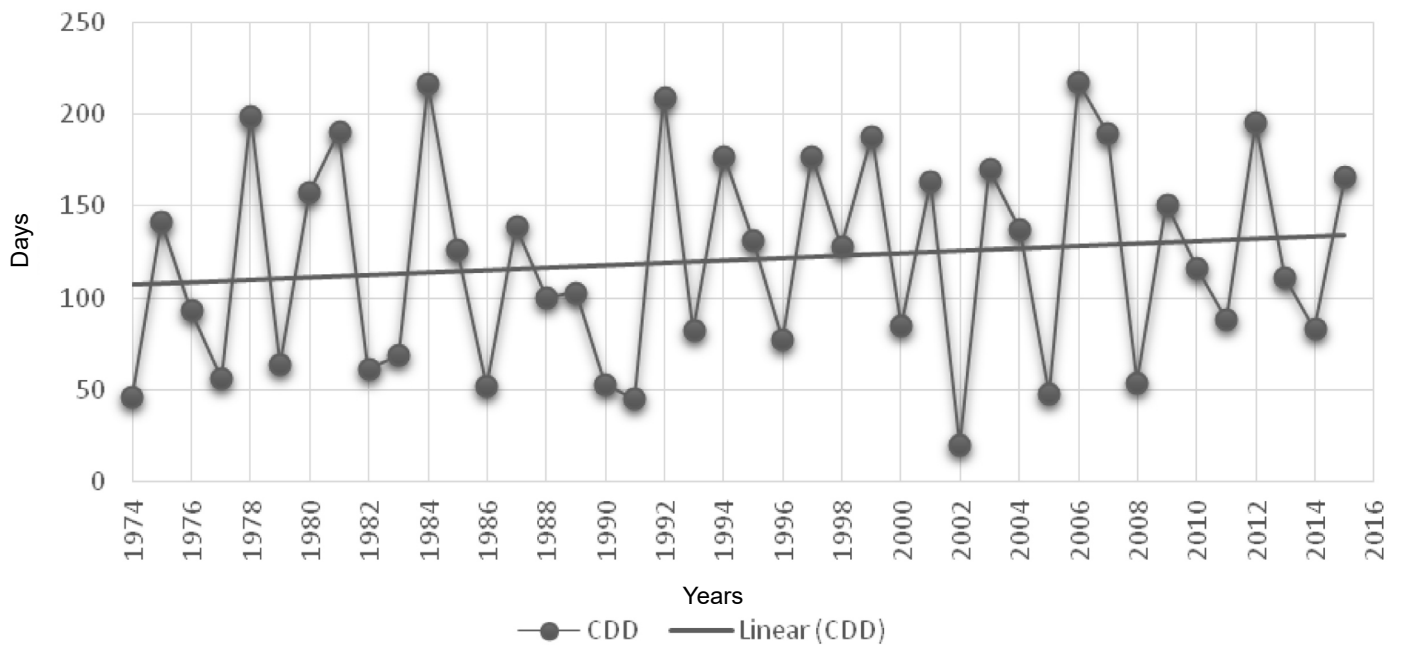


Figure 7 - Linear trend in the number of consecutive dry days (CDD) at the Aracati station (1974–2015).

The results found for Aracati station, unlike Trairi, show a trend of annual reduction in rainfall. In a study of the state of Ceará, Moncunill (2006) found negative trends in annual rainfall, using 23 pluviometric stations from 1974 to 2003. Santos et al. (2009), in a study of the entire state of Ceará, found results that point to a trend of increasing rainfall between 1935 and 2006.

Figure 7 shows the linear trend of the consecutive dry days (CDD) index for Aracati meteorological station from 1974 to 2015. There is a positive trend, indicating an increase in the number of consecutive dry days. The years 1984, 1992 and 2006 had more than 200 consecutive days without rain, that is, more than six months. The year 1993 was marked by a strong-intensity El Niño phenomenon, the most severe event of this magnitude recorded in the 1990s (Pereira et al., 2017; Rodrigues et al., 2017).

Linear trend of the number of consecutive dry days

This increase in consecutive days without rain is linked to the result of the index of total annual rainfall (PRCPTOT), presented above, since, with the decrease of the rainfall regime, there are fewer days with rain. This result indicates that, not only is it raining less in the region, but rainfall is increasingly sporadic, and is sometimes concentrated in a shorter period of time.

There is a great variability of rainfall, which often reaches peaks of four consecutive months or 120 days without precipitation. The year 2006 recorded the largest number of consecutive days without rain (217 days), that is, more than seven months.

Figure 8 shows the linear trend of the CDD index for the Trairi meteorological weather station, from 1976 to 2015. There is a negative trend, indicating a decrease in the number of consecutive dry days. The years 1982 and 1999 had more than 200 consecutive days without rain, that is, more than six months.

The divergent results between Aracati and Trairi pluviometric stations are justified by the divergence found in the calculation of the total annual precipitation index. When there is a decrease in the total annual rainfall, the days with rainfall tend to decrease as a consequence, generating an increase in the consecutive number of dry days and vice versa. Santos et al. (2009), who studied the state of Ceará, showed a variation between their pluviometric stations in the calculation of the CDD index, where there are both negative and positive trends in the number of consecutive dry days.

Linear trend in the number of consecutive days with rainfall > 1 mm

Figure 9 shows the trends of consecutive wet days (CWD) index of Aracati station (1974–2015). Considering the entire historical series, there was no trend of above increase or decrease as to the extreme climatic index of consecutive wet days, which corresponds to the maximum number of consecutive days in the year with rainfall above 1 mm. However, in recent years (2012–2015) there has been a reduction in the number of consecutive wet days.

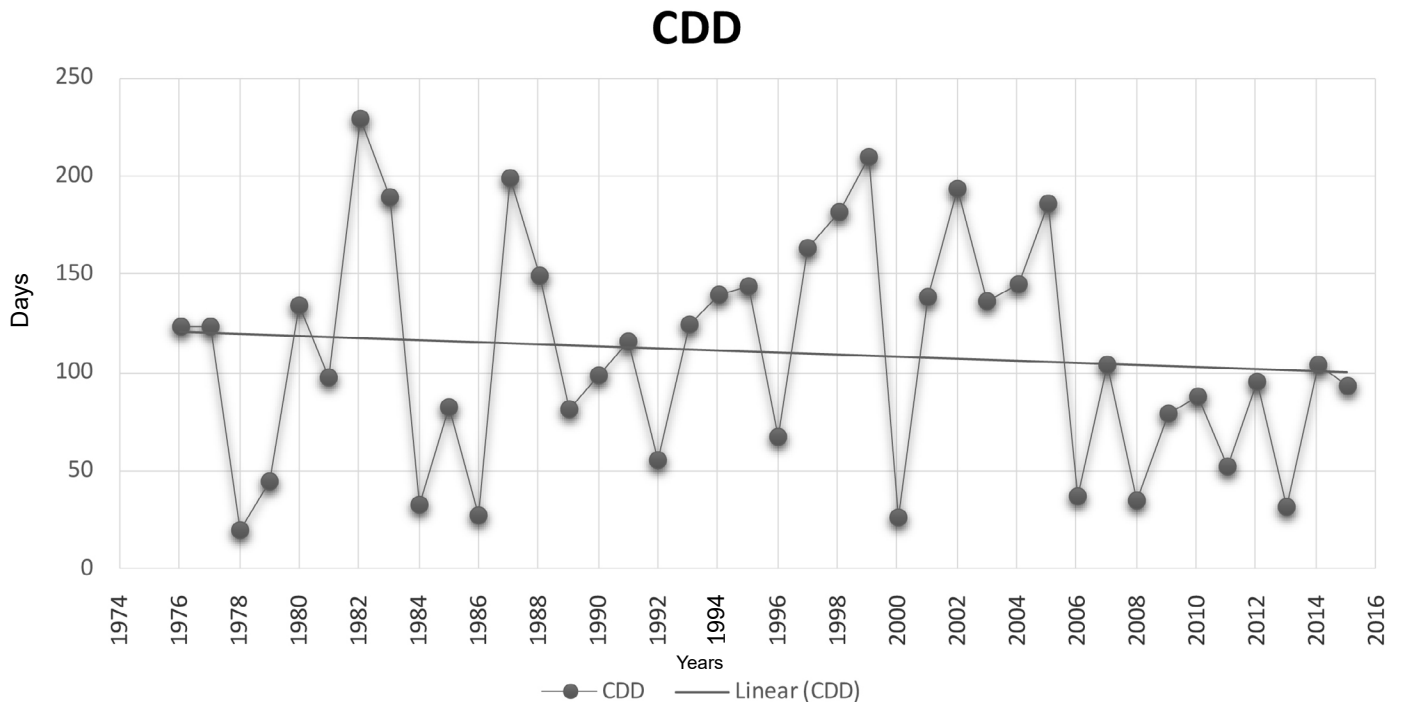


Figure 8 – Linear trend in the number of consecutive dry days (CDD) at the Trairi station (1976–2015).

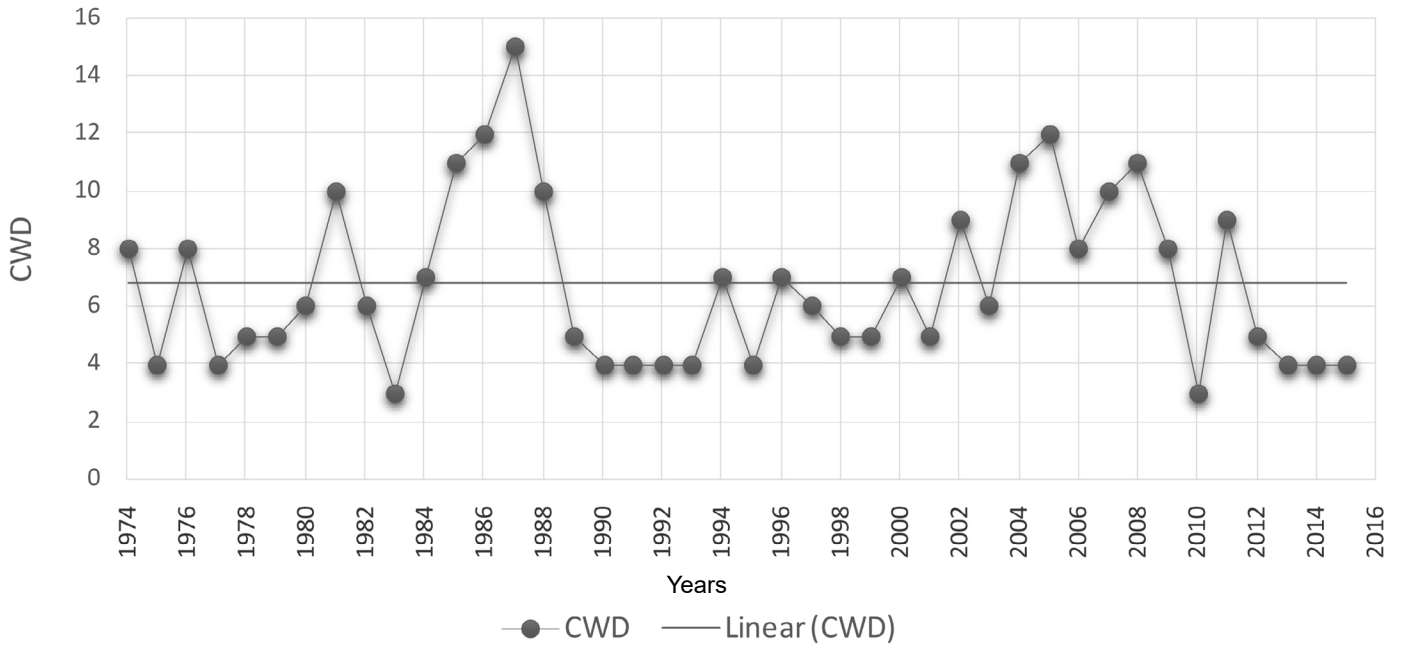


Figure 9 - Linear trend of the number of consecutive wet days (CWD) at the Aracati station (1974–2015).

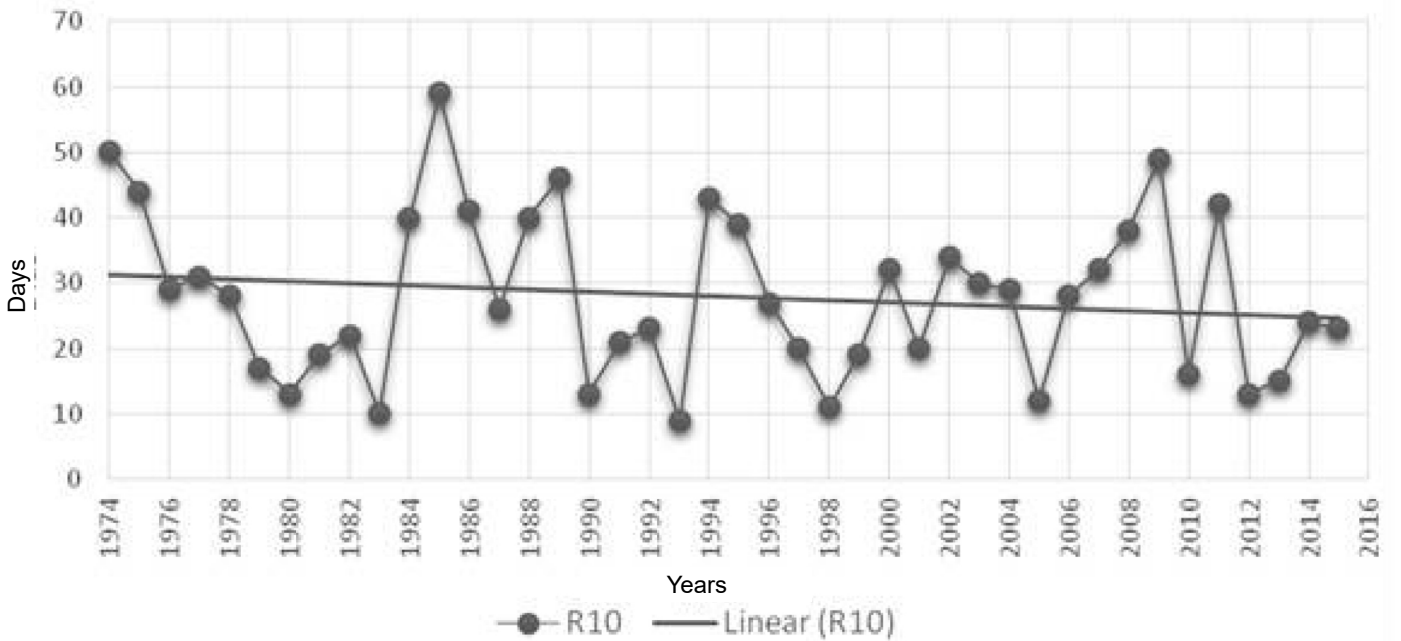


Figure 10 - Linear trend in the number of days/year in which rainfall was ≥ 10 mm (R10mm) at the Aracati station (1974–2015).

Figure 10 shows the linear trend of the extreme climate index R10mm at Aracati station, which represents the number of days per year in which rainfall was greater than 10 mm. The years 1985 and 2009 were those with the highest peaks; in these years, there were 59

and 49 days, respectively, when rainfall exceeded 10 mm. There is a linear trend to reduce the number of days with rainfall above 10 mm.

For the Trairi station, the analysis of the linear trend of the extreme climate index R10mm (Figure 11) shows that the years 1977,

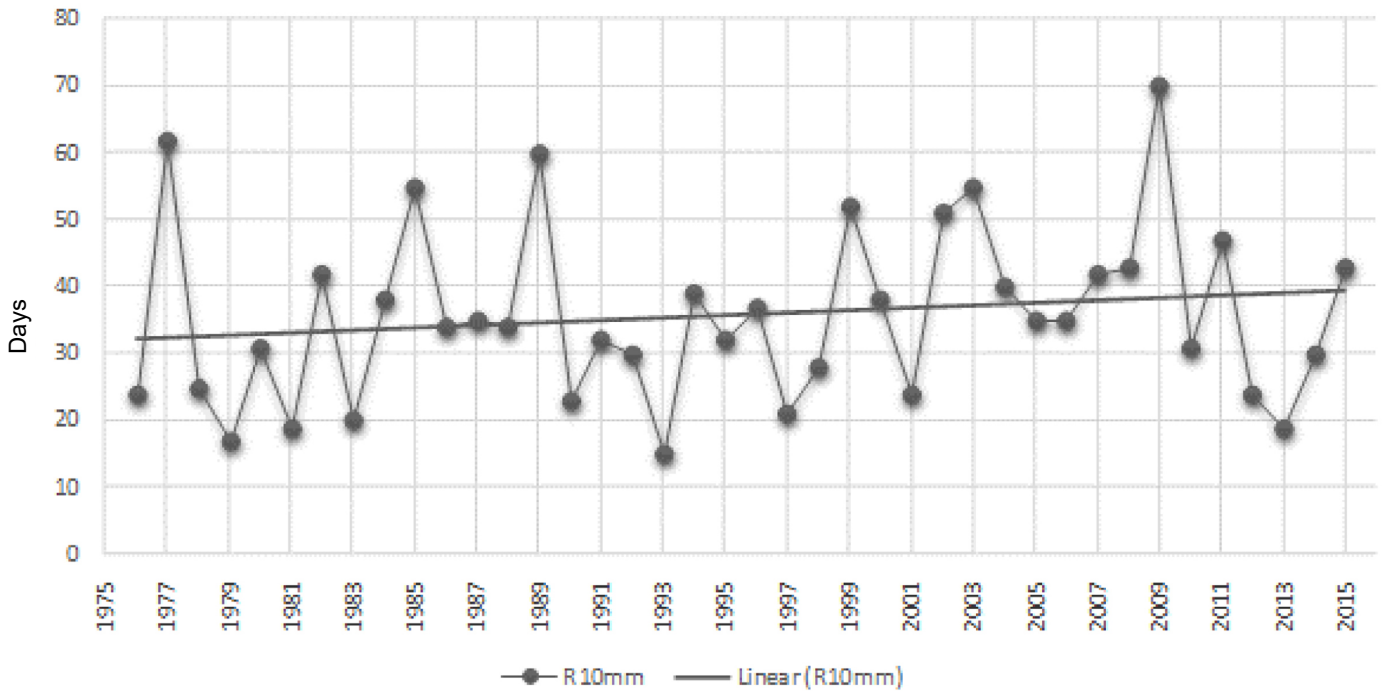


Figure 11 – Graph of the linear trend of the number of days/year in which rainfall was ≥ 10 mm (R10mm) at the Trairi station (1976–2015).

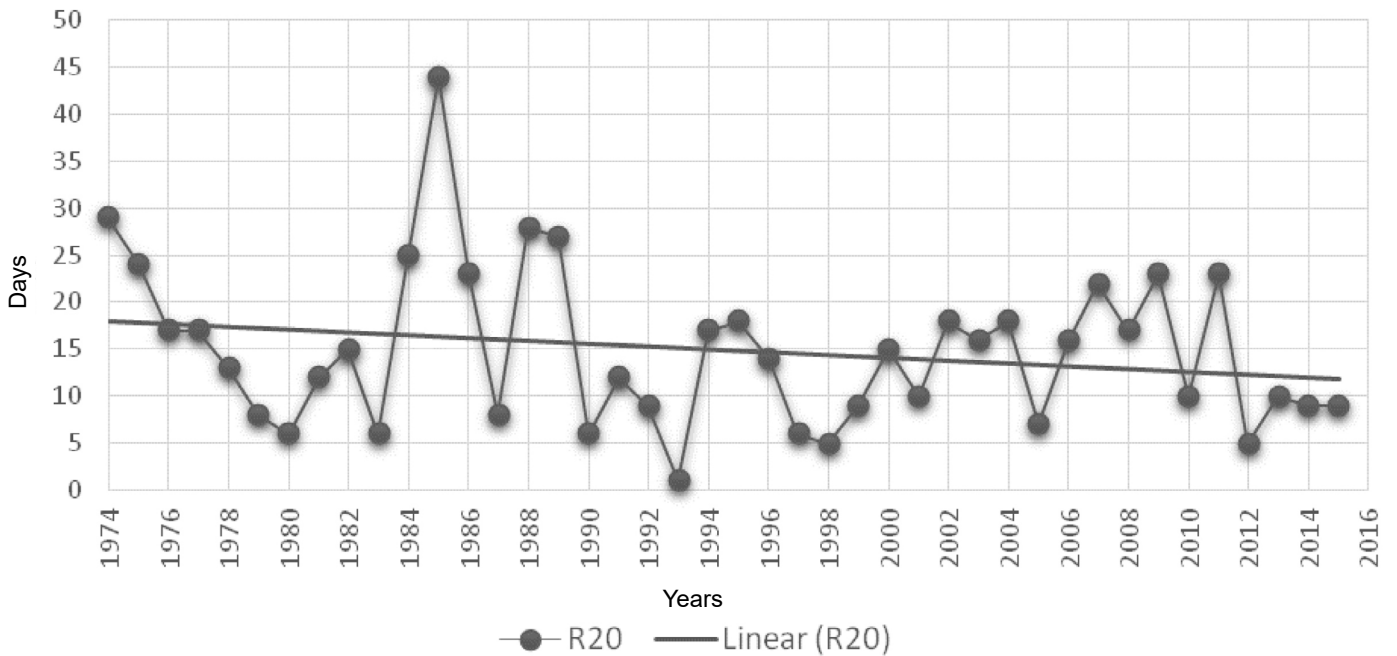


Figure 12 – Graph of the linear trend of the number of days/year in which rainfall was ≥ 20 mm (R20mm) at the Aracati station (1974–2015).

1989, and 2009 had the highest peaks; in these years, there were 60 and 70 days, respectively, in which rainfall exceeded 10 mm. There is a linear increasing trend in the number of days with rainfall above 10 mm.

Linear trend of number of days with rainfall > 20 mm

The R20mm index for the Aracati station (Figure 12) showed similar trends to the R10mm index, one of the biggest peaks during the first half of the historical series. From 2012 to 2015,

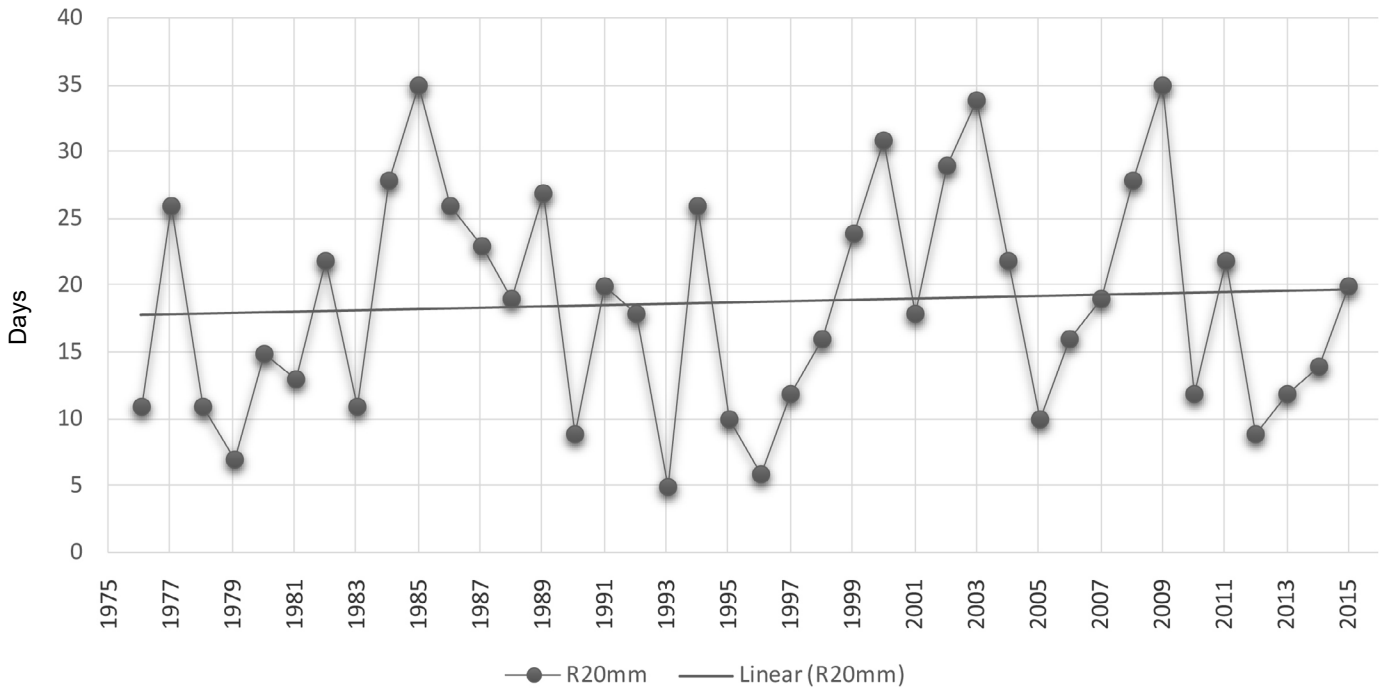


Figure 13 – Graph of the linear trend of the number of days/year in which rainfall ≥ 20 mm (R20mm) at the Trairi station (1976–2015).

the number of days with rainfall above 20 mm ranged from five to ten days.

For the Trairi station, the linear trend of the R20mm index (Figure 13) was also similar to that observed for the R10mm index. From 2012 to 2014, the number of days with rainfall above 20 mm was below average, varying from nine to 14 days.

Corroborating with the results previously shown, concerning the PRCPTOT and CDD climate indices, the analysis is consistent, since Aracati, which presented a decrease in rainfall and an increase in dry days, showed a decreasing trend in the number of days with rainfall up to 10 mm and up to 20 mm. The opposite occurred with Trairi, since, in this location, positive and negative trends were found for the PORCPTOT and CDD indices, consecutively.

Linear trend of the number of days with rainfall > 50 mm

The linear trend of the R50mm index at Aracati and Trairi stations (Figures 14 and 15) showed trends similar to the R10mm and R20mm indices.

For the Aracati station, the biggest peaks occurred during the first half of the historical series. The years 1985 and 2009 showed 11 and nine days, respectively, with rainfall above 50 mm. For Trairi station, the biggest peaks occurred during the second half of the historical series. The years 2000, 2003, and 2009 presented 11, 10 and nine days, respectively, with rainfall above 50 mm.

In the analysis of the indices of climatic extremes R10mm, R20mm, and R50mm, negative trends are observed in the three indices for the Aracati station, and positive trends for the Trairi station. For both stations, values below the historical average were recorded in the last four years, indicating that there was a decrease in the number of days per year with rainfall greater than 10 mm, 20 mm, and 50 mm, respectively. These indices are directly associated with the previous indices (PRCPTOT, CDD and CWD), since the results presented show a decrease in rainfall, an increase in the number of consecutive days without rain, and a decrease in the number of consecutive days with rain.

Linear trend of maximum rainfall in one day and five consecutive days

Analyzing the RX1day and RX5day indices at the Aracati station (Figures 16 and 17), there is neither a negative nor a positive trend. These indices correspond to the maximum rainfall recorded in one day and in five consecutive days, respectively. RX1day and RX5day are consistent with the PRCPTOT and R50mm indices, since there is a decreasing trend for both total rainfall and the number of days with heavy rain. Consequently, there is a decrease in these indices, both concentrated in one day and in five consecutive days.

Regarding the Trairi station, RX1day and RX5day indices (Figures 18 and 19) showed a slight negative trend, that is, a decrease in the maximum rainfall volume in one day and in five consecutive days,

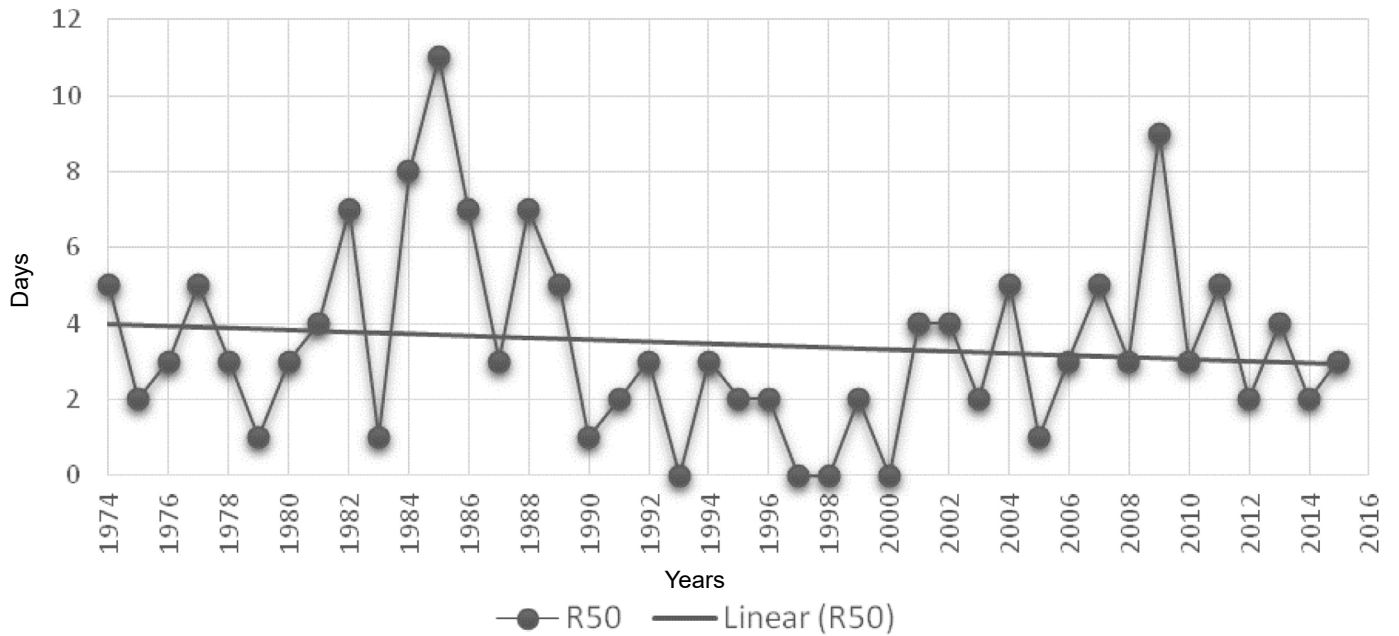


Figure 14 - Linear trend of the number of days/year in which rainfall was ≥ 50 mm (R50mm) at the Arcati station (1974–2015).

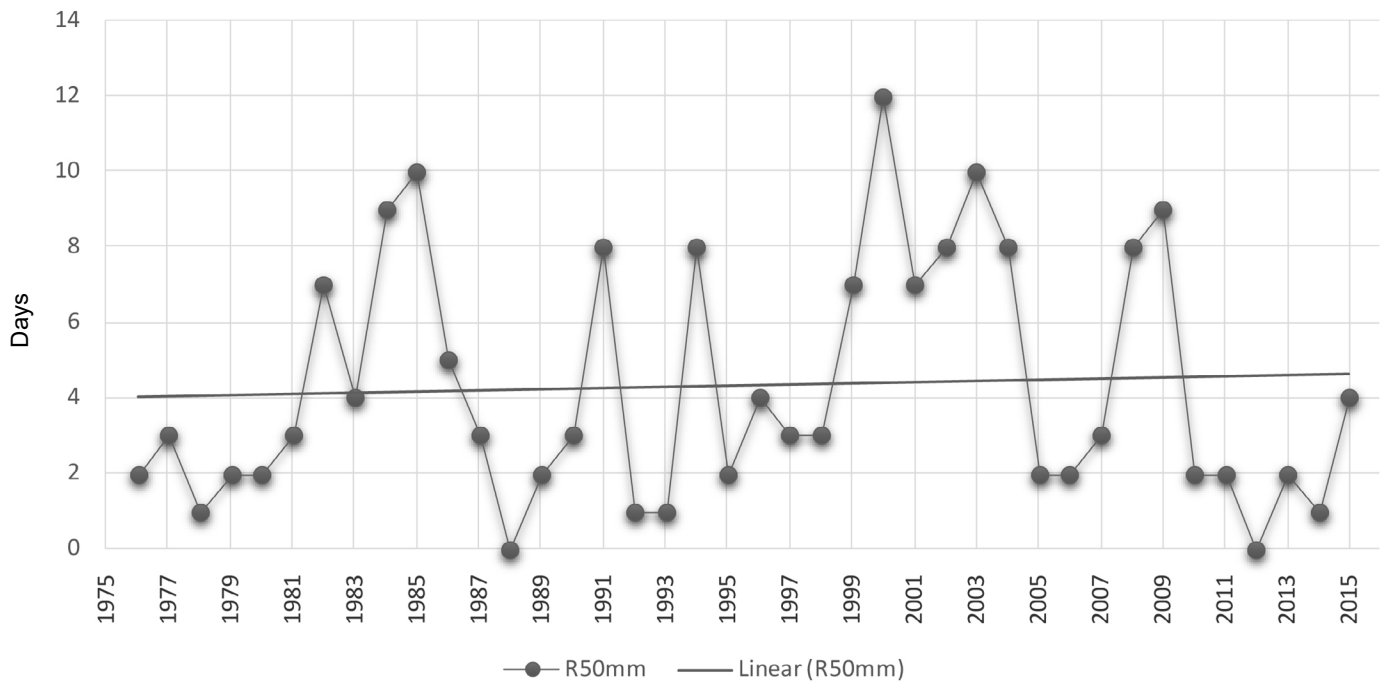


Figure 15 - Linear trend of the number of days/year in which rainfall was ≥ 50 mm (R50mm) at the Trairi station (1976–2015).

respectively. The maximum rainfall recorded in one day was 190 mm, and it occurred in 1976.

The predominance of negative trends in RX1day and RX5day indices shows a decrease in the maximum volume of rainfall in one day and

in five consecutive days. The predominance of negative trends in these indices reinforces the decreasing trends found in total rainfall, the decrease in the daily intensity of rainfall and the decrease in the number of days with heavy, moderate, and intense rainfall.

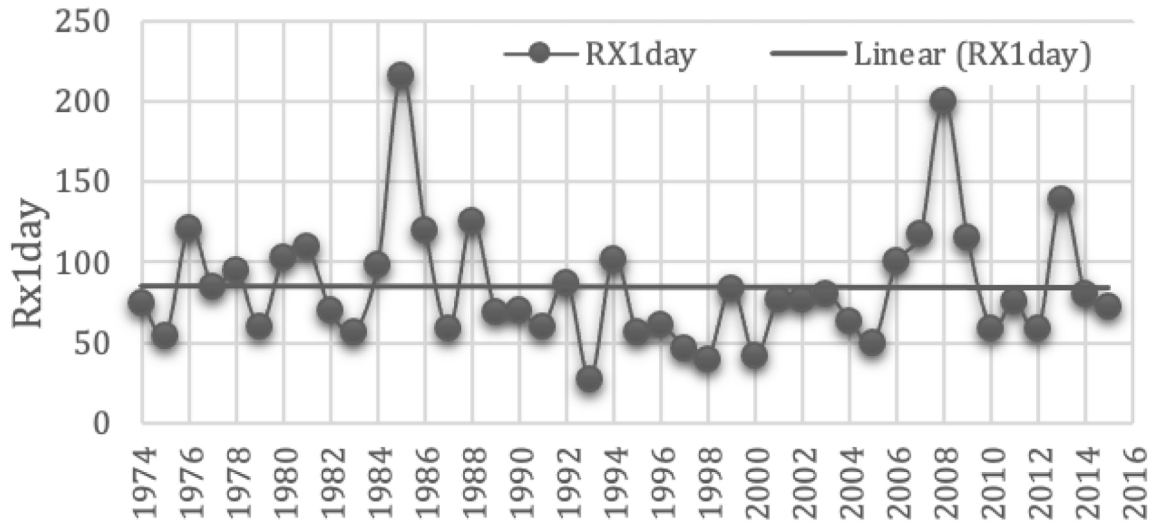


Figure 16 - Linear trend of the extremely humid days (RX1day) of the Aracati station (1974–2015).

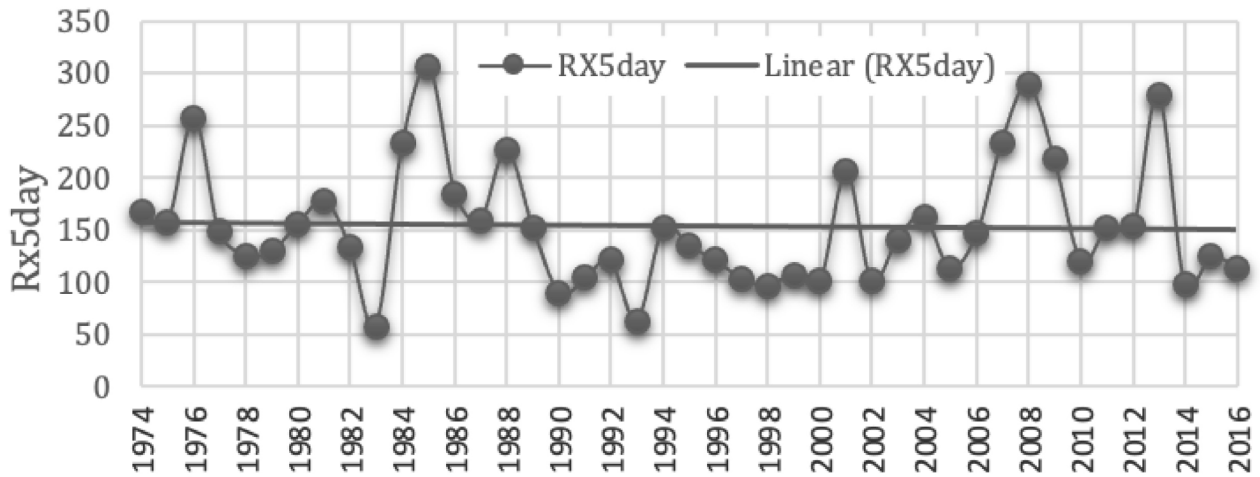


Figure 17 - Linear trend of the RX5day index of the Aracati station (1974–2015).

Considering the entire period of analysis for rainfall indices, there are few occurrences of significant trends of increase or decrease in the analyzed stations. However, it is clear that this result corroborates the work of Sillmann et al. (2013b), in which minor changes in rainfall rates for South America are present.

Analyzing the common period of rainfall and wind generation data from 2011 to 2015, the lowest capacity factor of wind generation is observed in 2011. In this same year, there was an increase in the number of consecutive wet days, as well as an increase in the number of days with rainfall above 10, 20, and 50 mm. However, from 2012 to 2015, capacity factors are higher and the exact opposite occurred, that is,

there was a reduction in the number of consecutive wet days and in the number of days with rainfall above 10, 20, and 50 mm.

Final Considerations

The analysis of the climatic extremes indices carried out for the rainy seasons of Trairi and Aracati, located in the state of Ceará, revealed a predominance of negative decreasing trends in total rainfall, showing that rainfall is increasingly scarce and concentrated in a shorter period of time, as indicated by the CDD and R50mm indices.

In the analysis of the climatic extremes indices R10mm, R20mm, and R50mm, negative trends are observed in the three indices for the

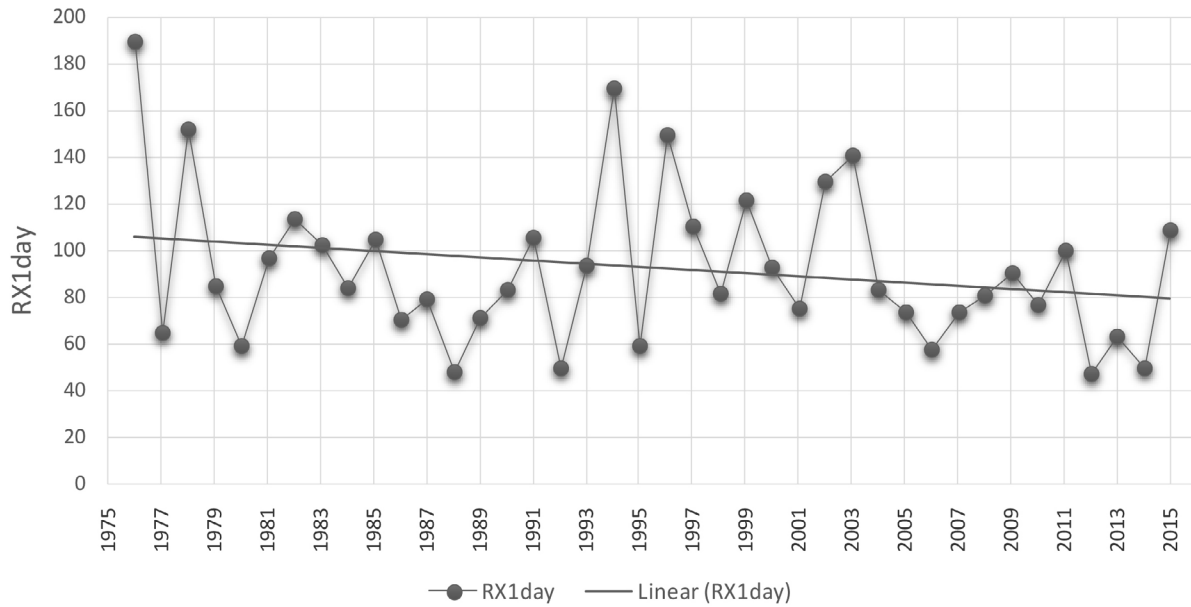


Figure 18 – Linear trend of the RX1day index of the Trairi station (1976–2015).

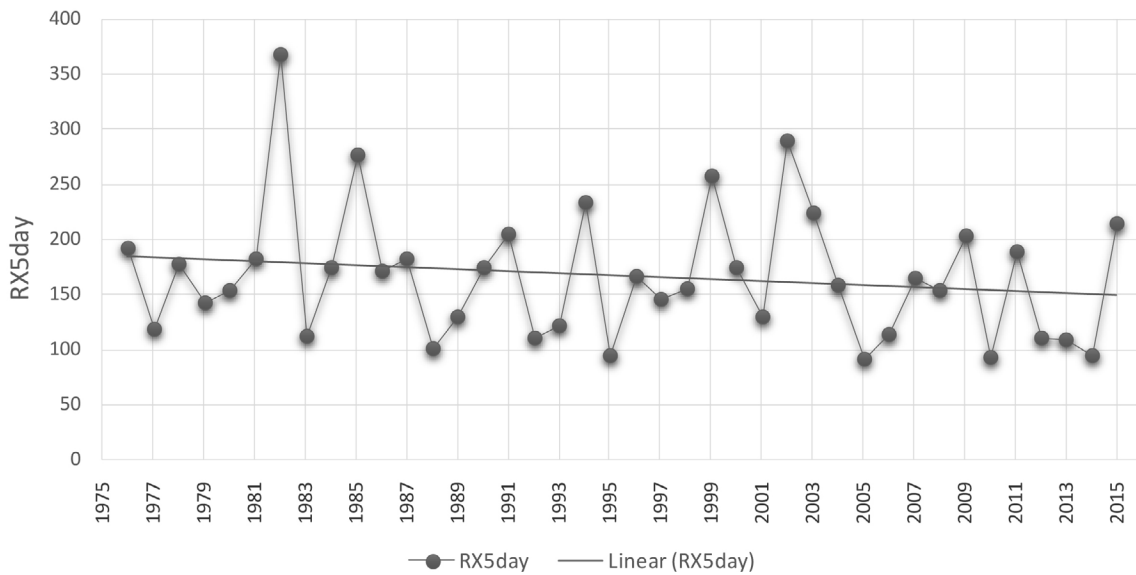


Figure 19 – Linear trend of the RX5day index of the Trairi station (1976–2015).

Aracati station, and positive trends for the Trairi station. For both stations, values below the historical average were recorded in the last four years, indicating that there was a decrease in the number of days per year with rainfall greater than 10 mm, 20 mm, and 50 mm, respectively. These indices are directly associated with the previous indices (PRCP-TOT, CDD and CWD), since the results presented show a decrease in rainfall, an increase in the number of consecutive days without rain, and a decrease in the number of consecutive days with rain.

Analyzing the common period of rainfall and wind generation data from 2011 to 2015, the lowest capacity factor of wind generation is observed in 2011. In this same year, there was an increase in the number of consecutive wet days, as well as an increase in the number of days with rainfall above 10, 20, and 50 mm. However, from 2012 to 2015, capacity factors are higher and the exact opposite occurred, that is, there was a reduction in the number of consecutive wet days and in the number of days with rainfall above 10, 20, and 50 mm. Thus, the period

of negative rainfall anomalies showed high wind generation capacity factors that may be associated with the occurrence of rainfall below the region's historical average, with extremely dry years.

For the analyzed period, there was an inversely proportional relationship between the rain anomaly index and the capacity factor of generation of the wind farm CE2, located close to the Aracati rain station, indicating that, in the months with negative precipitation anomalies, there was an increase in the capacity factor of wind generation in the months with negative rainfall anomalies. Due to the short history period of available data on verified wind generation, the need to repeat the analyzes for a period with a longer history is emphasized. For this region, verified wind generation data start in 2010.

In view of the climatic forecast of increased extreme weather events in the Northeastern region of Brazil, the present study must be expanded to other wind farms in the state of Ceará, as well as in different geographical regions and complex terrains, such as the states of Bahia, Rio Grande do Norte, Pernambuco, and Piauí. The results presented in research cannot be generalized for the entire Northeast,

since it was applied only to stations in the state of Ceará, with a reduced historical series.

The growing participation of wind generation in the Brazilian energy matrix, specifically in the Northeastern region, requires further studies aimed at improving the forecast of wind energy generation for other regions in different horizons. Therefore, with the accomplishment of this work, we expect to contribute to the scientific society, mainly to Brazil and specifically to the Northeast, with a greater understanding and detailing of the trends of extreme climatic indices of rainfall and its relation with wind energy generation.

Acknowledgements

We thank the professionals of the following institutions: Universidade Federal de Pernambuco, Operador Nacional do Sistema Elétrico, Empresa de Pesquisa Energética, Agência Nacional de Águas, Instituto Nacional de Meteorologia, Fundação Cearense de Meteorologia e Recursos Hídricos, who contributed by providing data, information and clarification.

Contribution of authors:

BARROS, A.M.L.: Conceptualization, Methodology, Validation, Formal analysis, Investigation, Resources, Data curation, Writing – original draft; SOBRAL, M.C.: Conceptualization, Methodology, Writing – original draft, review & editing; SOUZA, W.M.: Methodology, Analysis, Investigation, Validation; ASSIS, J.M.O.: Methodology, Data curation, Software, Validation.

References

- Araújo, L.E.; Moraes Neto, J.M.; Sousa, F.A.S., 2009. Análise Climática da Bacia do rio Paraíba – índice de Anomalia de Chuva (IAC). *Revista de Engenharia Ambiental*, v. 6, (3), 508-523.
- Assis, J.M.O.; Souza, W.M.; Sobral, M.C., 2015. Análise climática da precipitação no submédio da bacia do rio São Francisco com base no índice de anomalia de chuva. *Revista Brasileira de Ciências Ambientais*, (36), 115-127. <https://doi.org/10.5327/Z2176-947820151012>.
- Barros, A.M.L.; Machado, C.O.; Camargo, H.J.; Nascimento, P., 2017. Wind Power Forecasting Performed by Operador Nacional do Sistema Elétrico – ONS. In: 16th International Wind Integration Workshop. Berlin, Germany.
- Brasil. Agência Nacional de Águas (ANA). Hidroweb rainfall data (Accessed April 16, 2016) at: <http://hidroweb.ana.gov.br/>.
- Brasil. Ministério de Minas e Energia (MME). Empresa de Pesquisa Energética (EPE). Plano decenal de expansão de energia 2008/2017. 2009. EPE, Rio de Janeiro.
- Brasil. Ministério do Meio Ambiente. Secretaria de Biodiversidade e Florestas. Diretoria de Conservação da Biodiversidade. 2007. Relatório 5. Mudanças Climáticas Globais e Efeitos sobre a Biodiversidade - Subprojeto: Caracterização do clima atual e definição das alterações climáticas para o território brasileiro ao longo do século XXI. Ministério do Meio Ambiente, Brasília.
- Carvalho, A.T.F., 2020. Caracterização climática da quadra chuvosa em Apodi, semiárido brasileiro, nos anos de 2013 a 2017. *Revista Geografia em Atos*, v. 2, (17), 4-23. <https://doi.org/10.35416/geoatos.v2i17.7116>.
- Coelho, C.A.S.; Cardoso, D.H.F.; Firpo, M.A.F., 2016. Precipitation diagnostics of an exceptionally dry event in São Paulo, Brazil. *Theoretical and Applied Climatology*, v. 125, (3-4), 769-784. <https://doi.org/10.1007/s00704-015-1540-9>.
- Custódio, R.S., 2009. Energia Eólica para produção de Energia Elétrica. Eletrobras, Rio de Janeiro.
- Espinoza, J.C.; Marengo, J.A.; Ronchail, J.; Carpio, J.M.; Flores, L.N.; Guyot, J.L., 2014. The extreme 2014 flood in south-western Amazon basin: the role of tropical subtropical South Atlantic SST gradient. *Environmental Research Letters*, v. 9, (12), 1-9. <https://doi.org/10.1088/1748-9326/9/12/124007>.
- Espinoza, J.C.; Ronchail, J.; Frappart, F.; Lavado, W.; Santini, W.; Guyot, J.L., 2013. The major floods in the Amazonas river and tributaries (Western Amazon basin) during the 1970–2012 period: a focus on the 2012 flood. *Journal of Hydrometeorology*, v. 14, (3), 1000-1008. <https://doi.org/10.1175/JHM-D-12-0100.1>.
- Ferreira, A.G.; Mello, N.G.S., 2005. Principais Sistemas Atmosféricos Atuantes sobre a Região Nordeste do Brasil e a sua Influência dos Oceanos Pacífico e Atlântico no Clima da Região. *Revista Brasileira de Climatologia*, v. 1, (1), 2005.
- Ferreira, P.S.; Gomes, V.P.; Galvêncio, J.D.; Santos, A. M.; Souza, W.M., 2017. Avaliação da tendência espaço-temporal da precipitação pluviométrica em uma região semiárida do estado de Pernambuco. *Revista Brasileira de Climatologia*, v. 21, 113-134. <https://doi.org/10.5380/abclima.v21i0.45895>.
- Figueiredo Filho, D.B.; Silva Júnior, J.A., 2009. Desvendando os Mistérios do Coeficiente de Correlação de Pearson (r). *Revista Política Hoje*, v. 18, (1).

- Freitas, M.A.S., 2005. Um Sistema de Suporte à Decisão para o Monitoramento de Secas Meteorológicas em Regiões Semi Áridas. *Revista Tecnologia*, suppl., p. 84-95.
- Global Wind Energy Council (GWEC). 2010. Global Wind Report: Annual market Update (Accessed June 12, 2015) at: http://gwec.net/wp-content/uploads/2012/06/GWEC_annual_market_update_2010_-_2nd_edition_April_2011.pdf.
- Global Wind Energy Council (GWEC). 2016. Global Wind Report (Accessed May 20, 2016) at: http://www.gwec.net/wp-content/uploads/vip/GWEC_PRstats2016_EN_WEB.pdf.
- Instituto Brasileiro de Geografia e Estatística (IBGE). 2011. Cartas e mapas (Accessed Sept 5, 2020) at: https://geofp.ibge.gov.br/cartas_e_mapas/
- Karl, T.R.; Nicholls, N.; Ghazi, A., 1999. CLIVAR/GCOS/WMO workshop on indices and indicators for climate extremes: workshop summary. *Climatic Change*, 42, 3-7.
- Koch, H.; Silva, A.N.C.; Azevedo, J.R.G.; Souza, W.M.; Köppel, J.; Souza Junior, C.B.; Barros, A.M.L.; Hattermann, E., 2018. Integrated hydro- and wind power generation: a game changer towards environmental flow in the Sub-middle and Lower São Francisco River Basin? *Regional Environmental Change*, v. 1, 1927-1942. <https://doi.org/10.1007/s10113-018-1301-2>.
- Lewis, S.L.; Brando, P.M.; Phillips, O.L.; Van Der Heijden, G.M.; Nepstad, D., 2011. The 2010 Amazon Drought. *Science*, v. 331, (6017), 554. <https://doi.org/10.1126/science.1200807>.
- Luz, C.; Vasconcelos, E.; Bilotta, P.; Carvalho Filho, M.A., 2020. Avaliação dos impactos ambientais em parques eólicos offshore e onshore utilizando a matriz de leopold. *Revista Brasileira de Ciências Ambientais* (Online), 55, (2), 206-225. <https://doi.org/10.5327/Z2176-947820200644>.
- Lyra, M.J.A.; Cavalcante, L.C.V.; Levit, V.; Fedorova, N., 2019. Ligação Entre Extremidade Frontal e Zona de Convergência Intertropical Sobre a Região Nordeste do Brasil. *Anuário do Instituto de Geociências*, v. 42, (1), 413-424. https://doi.org/10.11137/2019_1_413_424.
- Marengo, J.A., 2007. Mudanças climáticas globais e seus efeitos sobre a biodiversidade: caracterização do clima atual e definição das alterações climáticas para o território brasileiro ao longo do século XXI. 2. ed. Ministério do Meio Ambiente, Brasília, v. 1.
- Marengo, J.A., 2008. Água e mudanças climáticas. *Estudos Avançados*, v. 22, (63), 83-96. <https://doi.org/10.1590/S0103-40142008000200006>.
- Marengo, J.A.; Cunha, A.P.; Alves, L.M., 2016. A seca de 2012-15 no semiárido do Nordeste do Brasil no contexto histórico (Accessed September 4, 2020) at: https://www.researchgate.net/publication/311058940_A_seca_de_2012-15_no_semiarido_do_Nordeste_do_Brasil_no_contexto_historico.
- Marengo, J.A.; Tomasella, J.; Soares, W.R.; Alves, L.M.; Nobre, C.A., 2012. Extreme climatic events in the Amazon basin climatological and hydrological context of recent floods. *Theoretical and Applied Climatology*, v. 107, (1-2), 73-85. <https://doi.org/10.1007/s00704-011-0465-1>.
- Moncunill, D.F., 2006. The rainfall trend over Ceará and its implications. In: 8ª Conferência Internacional de Meteorologia e Oceanografia do Hemisfério Sul. Foz do Iguaçu, 315-323.
- Munichre. 2017. Münchener Rückversicherungs-Gesellschaft. Natural catastrophes 2016 - Analysis, assessments, positions. Munichre, München, 80 pp.
- Oliveira, J.L.; Costa, A.A., 2011. Estudo da variabilidade do vento em escala sazonal sobre o Nordeste brasileiro utilizando o RAMS: os casos de 1973-1974 e 1982-1983. *Revista Brasileira de Meteorologia*, v. 26, (1), 95-108. <https://doi.org/10.1590/S0102-77862011000100006>.
- Operador Nacional do Sistema Elétrico (ONS). 2020. Plano da Operação Energética 2020/2024 - PEN 2020. DPL-REL-0195-2020_PEN. Condições de Atendimento. v. 1 (Accessed on July 31, 2020) at: <https://sintegre.ons.org.br/sites/8/43/76/paginas/servicos/produtos.aspx>.
- Pereira, M.L.T.; Soares, M.P.A.; Silva, E.A.; Montenegro, A.A.A.; Souza, W.M., 2017. Variabilidade climática no Agreste de Pernambuco e os desastres decorrentes dos extremos climáticos. *Journal of Environmental Analysis and Progress*, v. 2, (4), 394-402. <https://doi.org/10.24221/jeap.2.4.2017.1452.394-402>.
- RCLIMDEX 1.0. 2004. Manual Del Usuario (Accessed June 12, 2015) at: <http://etccdi.pacificclimate.org/software.shtml>.
- Reeves, B.A.; Beck, F., 2003. Wind Energy for Electric Power - Technical Report for Renewable Energy Policy Project.
- Ribeiro, F.; Ferreira, P.; Araújo, M.; Braga, A.C., 2014. Public opinion on renewable energy technologies in Portugal. *Energy*, v. 69, 39-50. <https://doi.org/10.1016/j.energy.2013.10.074>.
- Rodrigues, L.O.; Souza, W.M.; Costa, V.S.O.; Pereira, M.L.T., 2017. Influência dos eventos de El Niño e La Niña no regime de precipitação do Agreste de Pernambuco. *Revista Brasileira de Geografia Física*, v. 10, (6), 1995-2009. <https://doi.org/10.26848/rbfg.v10.6.p1995-2009>.
- Santos, C.A.C.; Brito, J.L.B.; Rao, T.V.R.; Menezes, H.E.A., 2009. Tendências dos índices de precipitação no estado do Ceará. *Revista Brasileira de Meteorologia*, v. 24, (1), 39-47. <https://doi.org/10.1590/S0102-77862009000100004>.
- Sillmann, J.; Kharin, V.V.; Zhang, X.; Zwiers, F.W.; Bronaugh, D., 2013a. Climate extremes indices in the CMIP5 multi-model ensemble. Part 1: Model evaluation in the present climate. *Journal of Geophysical Research: Atmospheres*, v. 118, (4), 1716-1733. <https://doi.org/10.1002/jgrd.50203>.
- Sillmann, J.; Kharin, V.V.; Zwiers, F.W.; Zhang, X.; Bronaugh, D., 2013b. Climate extremes indices in the CMIP5 multi-model ensemble. Part 2: Future climate projections. *Journal of Geophysical Research: Atmospheres*, v. 118, (6), 2473-2493. <https://doi.org/10.1002/jgrd.50188>.
- Souza, A.D., 2010. Avaliação da Energia Eólica para o Desenvolvimento Sustentável das Mudanças Climáticas no Nordeste do Brasil. Dissertation, Centro de Tecnologia e Geociências, Programa de Pós-Graduação em Engenharia Civil, Universidade Federal de Pernambuco, Recife.
- Souza, W.M.; Azevedo, P.V.; Assis, J.M.O.; Sobral, M.C.M., 2014. Áreas de risco mais vulneráveis aos desastres decorrentes das chuvas em Recife-PE. *Revista Brasileira de Ciências Ambientais*, (34), 79-94.
- Tucci, C.E.M., 2004. Hidrologia: Ciência e Aplicação. 3ª ed. Editora da UFRGS/ABRH, Porto Alegre, 943 pp.
- Van-Rooy, M.P., 1965. A Rainfall Anomaly Index Independent of Time and Space. *Notes*, v. 14, 43-48.
- Varejão-Silva, M.A., 2006. Meteorologia e Climatologia. Recife, 463 pp (Accessed May 13, 2017) at: https://icat.ufal.br/laboratorio/clima/data/uploads/pdf/METEOROLOGIA_E_CLIMATOLOGIA_VD2_Mar_2006.pdf.
- Wang, B.; Wang, Q.; Wei, Y.-M.; Li, Z.-P., 2018. Role of renewable energy in China's energy security and climate change mitigation: An index decomposition analysis. *Renewable and Sustainable Energy Reviews*, v. 90, 187-194. <https://doi.org/10.1016/j.rser.2018.03.012>.
- Zack, J.W.; Shiu, V.D.H.; Chen, S.H.; Chen, C.Y.; MacDonald, C., 2016. Impact of Targeted Measurements and Next-Generations Prediction Techniques on Short-Term Wind Ramps Forecasting in the Tehachapi Wind Resource Area. 15th Wind Integration Workshop, Vienna, Austria.